Solid Freeform Fabrication 2019: Proceedings of the 30th Annual International
Solid Freeform Fabrication Symposium – An Additive Manufacturing Conference
Reviewed Paper

MANUFACTURING OF NANOPARTICLE-FILLED PA11 COMPOSITE PARTICLES FOR SELECTIVE LASER SINTERING

Maximilian A. Dechet[#‡], Lydia Lanzl[†‡], Alisa Wilden[#], Maria-Melanie Sattes[#], Dietmar Drummer[†‡], Wolfgang Peukert[#‡], Jochen Schmidt[#‡]*

[#] Institute of Particle Technology (LFG), Friedrich-Alexander-Universität Erlangen-Nürnberg, Cauerstr. 4, D-91058 Erlangen

[†] Institute of Polymer Technology, Friedrich-Alexander-Universität Erlangen-Nürnberg, Am Weichselgarten 9, 91058 Erlangen, Germany

[‡] Collaborative Research Center 814 – Additive Manufacturing, Am Weichselgarten 9, D-91058 Erlangen, Germany

Abstract

Selective laser sintering (SLS) is an Additive Manufacturing (AM) process that yields excellent part qualities with good mechanical properties. The SLS process employs micron-sized polymer particles, which are selectively fused by a laser. While there seem to be hardly any boundaries regarding design, there are quite some restrictions concerning the variety of commercially available SLS materials. With a market share of roughly 90%, polyamide 12 (PA12) is currently the most widely used polymer material for SLS. Concerning particle or fiber enhanced materials, only dry blended, but hardly any composite materials are available.
In this contribution, the manufacturing of nanoparticulate alumina-, titania- and silica-filled polyamide 11 (PA11) particles is demonstrated. The particles are manufactured via liquid-liquid phase separation and precipitation (also known as solution-dissolution process) from ethanol dispersions. Bulk polymer material of PA11 is directly converted to composite microparticles in a one-pot approach. The produced particles are characterized regarding their size and morphology. The amount of nanoparticles in the bulk is assessed via thermogravimetric analysis (TGA). Furthermore, the effect of the nanoparticles as nucleating agents is investigated via DSC and correlated with surface energies as determined by inverse gas chromatography (IGC).

Introduction

The field of polymer-based Additive Manufacturing (AM) and its areas of application are constantly expanding. Technologies such as fused filament fabrication (FFF), stereolithography (SLA) or binder jetting enable 3D printing of a wide variety of components, whether flexible or rigid. However, if functional components with high strength and stability are required, typically powder-based AM technologies, above all laser powder bed fusion (aka selective laser sintering (SLS) are chosen. In this process, a homogeneous layer of powder is spread onto a building platform. The temperature in the manufacturing system is set between the onset of melting and the onset of crystallization of the respective polymer. This temperature range often is referred to as ‘sintering window’. The particles in the spread powder are selectively fused with a laser, according to the cross section of the part to be built in this layer, before the building platform is lowered by the height of one powder layer and the process is repeated. The SLS process offers a huge freedom of design, as no additional support structures are needed, due to the surrounding powder bed acting as support [1]. However, some limitations, especially concerning the functionality of the parts produced, stem from the limited choice of commercially available powder materials. With a market share of around 90%, polyamide 12 (PA12) is currently the most commonly used SLS powder material [2]. The reasons behind this lack of alternative materials are the demanding requirements needed for SLS processing. Applicable polymer powders must be optimized with regard to size, shape, flowability, packing properties, but also thermal and rheological properties. Thereby, new functionalities can either be introduced via development of novel powder materials based on polymers other than PA12, or by adding new functionalities to existing powder materials via fillers to obtain composites. Especially nanoparticles are known to add many new functionalities to plastics, from improvement of mechanical properties, to thermal or electrical conductivity, optical properties or changes in

rheological behavior, to only name a few [3–6]. Adnan et al. [7] could show a correlation between smaller filler size and increased elastic properties in nanocomposite materials, especially with homogeneously distributed nanoparticles. There are many methods and processes to obtain composite powders [8], among them melt compounding and ball milling [9], spray drying [10], solvent evaporation and physical mixing [11].

In this study, the precipitation, or solution-dissolution, process to manufacture composite powder materials is utilized. This process is used to manufacture the largest portion of commercial PA12 powders used in SLS [12,13]. It is based on the dissolution of the polymer in a so-called moderate solvent at elevated temperatures and subsequent cooling of the solution. During cooling, the system reaches a miscibility gap, where, dependent on the system composition and process parameters, thermally-induced liquid-liquid phase separation (TIPS) sets in. During TIPS, polymer-rich droplets form in a polymer-lean continuous solvent phase. Subsequently, the polymer in the droplets solidifies or crystalizes and polymer microparticles are obtained. The final size distribution and shape depend, among others, on the solvent-polymer system, the initial polymer concentration, droplet coalescence and Ostwald ripening, stirring conditions etc. More information on this process can be found in [14–19]. Concerning additive manufacturing with PA11-nanocomposites, Chung and Das [22] investigated the manufacturing of functionally graded PA11-silica nanocomposite parts via SLS. They prepared the composite material with 2-10 vol.% silica by blending a PA11 powder with the silica in a rotary tumbler. They reported a complex interplay between nanosilica volume fraction and tensile modulus, as the modulus decrease up to 4 vol.% silica, whereas from there the modulus increases again for up to 10 vol.% of silica, where the modulus reached its maximum value. Analogous behavior was also observed for the compressive modulus. The manufacturing of a PA11-alumina nanocomposite was reported by Warnakula and Singamneni [23], with the aim to employ the alumina as heat storage, as the alumina absorbs 96 % of the CO_2-laser wavelength and subsequently dissipates the energy slowly as heat in order to improve the sintering. They prepared composites with 1 wt.% to 10 wt.% alumina by physical mixing and manufactured thin layers via SLS, but did also observe a narrowing of the sintering window. The addition of titania during the solution-dissolution process for the manufacturing of SLS powders is patented by Evonik, where they claim an improved surface quality due to an increased yellowing resistance when exposed to thermal stress during SLS [24]. Furthermore, also improved mechanical properties, especially modulus of elasticity, are claimed. In a recent publication, we investigated the solution-dissolution process for the manufacturing of PA11 particles and performed a thorough particle and material characterization before applying the material in the SLS process [25]. As an extension of this work, in this study we investigate the manufacturing of nanoparticle-filled PA11 particles with tailored filler content and characterize them regarding their SLS processability. In addition to particle size and shape, the filler content is assessed via thermogravimetric analysis (TGA), while analysis of the incorporation of the fillers into the PA11 particles is performed via microscopy on epoxy-embedded and polished samples. Furthermore, the influence of the nanoparticles on the sintering window and their effect as nucleating agents is investigated via DSC and possible correlations with surface energies as determined by inverse gas chromatography (IGC) are studied. The investigated filler nanoparticles, namely silica, alumina and titania, are chosen as model systems, as silica could provide creep resistance and impact strength, titania UV-resistance and aging protection and alumina enhanced mechanical strength and increased laser absorption [8].

Materials

Polyamide 11 granules (Rilsan BMN O natural, Arkema) were used as feed material. Ethanol (99.5 %, denatured with 1 % MEK, VWR) was used as a moderate solvent without further purification. The nanoparticles used for filling the PA11 were pyrogenic silica (Aeroxide OX 50, Evonik), pyrogenic alumina (Aeroxide Alu C, Evonik) and pyrogenic titania (Aeroxide TiO_2 T 805, Evonik).

Methods

Precipitation of filled PA11 particles

DAB-3 (Berghof) steel autoclaves equipped with PTFE liners placed on stirrer hotplates were used as reactors for particle manufacturing. A detailed description of the particle precipitation procedure can be found in [25]. In all reported experiments 20 g PA11 granules and 80 g ethanol were used. The added nanoparticle concentrations are given as weight fraction with respect to the polymer mass. To ensure proper dispersion of the nanoparticles in the solvent, the appropriate amount of nanoparticles was mixed with ethanol and dispersed for 15 min using a rotor-stator mixer (Ultra Turrax T18, IKA). The autoclaves were then heated to 190 °C, where the system was held for 15 min, to ensure complete dissolution of the PA11, before heating was turned off. The system was then cooled to 130 °C where an isothermal step was applied for 30 min. Stirring inside the autoclaves was realized via magnetic stirring bars (6mm x 25 mm) and varied between 100 and 600 rpm for the silica and alumina systems. For the titania systems, the dispersion was not stable when stirred with 100 rpm, therefore stirring was varied between 300 and 1200 rpm. The autoclaves were opened at temperatures below 60°C and the product particles were collected by filtration via a Büchner funnel (Grade 1 filter, Whatman). The recovered wet particles were subsequently dried in an oven.

Laser diffraction particle sizing

Particle size distribution (PSDs) of the nanoparticle-filled PA11 was measured by laser diffraction using a Mastersizer 2000 equipped with a Scirocco 2000 dry dispersion unit (Malvern). The dispersion gas pressure was 2 bar.

Scanning Electron Microscopy (SEM) and energy dispersive X-ray spectroscopy (EDX)

Shape and surface morphology of the PA11 particles were characterized by scanning electron microscopy (SEM) with a GeminiSEM 500 (Carl Zeiss) operated at an acceleration voltage of 1.0 kV. A secondary electron detector was used for imaging. Elemental analysis of the nanofillers was conducted by energy dispersive X-ray spectroscopy (EDX) (X-Max, 80 mm², Oxford Instruments).

Differential scanning calorimetry (DSC)

Differential scanning calorimetry (DSC) for the nanoparticle-filled PA11 powders was performed using a DSC8000 (PerkinElmer). The samples were placed in standard aluminum pans with covers and measured at a heating rate of 10 K/min from 30°C to 210°C followed by cooling to 30°C at 10 K/min. Measurements were conducted under continuous nitrogen purge gas flow (25 mL/min).

Thermogravimetric analysis (TGA)

Determination of the integral nanoparticle content in the filled PA11 powders was realized by assessing the weight of the ash residue via TGA. Experiments were performed in synthetic air using a TGAQ50 (TA Instruments). A ceramic pan with a volume of 250 µl was used and the sample weight was approximately 30-50 mg. Measurements were conducted in a temperature range of 30–900 °C with a heating rate of 10 K/min.

Particle cross-section inspection

In order to analyze the filler distribution and the location of the fillers within the polymer particles, polished cross-sections of the particles are evaluated by electron microscopy. The powder particles are embedded in epoxy, before the samples are grinded and polished. Thereby, the inner volume of the particles is accessible, which allows for investigation of filler presence in the particle volume. The polished sections are then analyzed via SEM (Ultra Plus, Carl Zeiss) at 10 kV for high resolution imaging of the nano-fillers. Via an energy dispersive X-ray (EDX)-elemental analysis, the chemical identity of the nano-fillers can be assessed.

Inverse gas chromatography (IGC)

The measurements of inverse gas chromatography (IGC) were conducted using a Surface Energy Analyzer (Surface Measurement Systems). Each sample was filled into a 6 mm x 30 mm (inner diameter 3 mm) sample column with sample weights between 13 and 68 mg, providing about 1 m² of sample surface area. After conditioning the samples at 80 °C for two hours, surface energies were measured at 50 °C. Heptane, octane and nonane were used to determine the dispersive surface energies, while toluene and dichloromethane were used for the acid-base properties.

Results

To study the influence of the type and concentration of the added nanoparticles present in the moderate solvent during precipitation, experiments with varying concentrations of added nanoparticles were conducted. For titania and silica, precipitation experiments up to 30 wt.% of filler could be performed. For alumina, it was not possible to disperse more than 10 wt.% (≙ 2 g) in 80 g of ethanol, due to the low dispersion stability. The particle size distributions of alumina-filled, silica-filled and titania-filled PA11 particles are depicted in Figure 1. Compared to the sample without any fillers, the added nanoparticles neither strongly increase, nor decrease the particle size of the product. For the 30 wt.% silica sample however, a pronounced sub 10 µm fine fraction could be observed. While all samples show some fine and coarse fraction outside the specification of typical SLS powders, their use in SLS could be easily provided by appropriate classification (e.g. sieving). Furthermore, no general trend correlating particle size with increasing nanoparticle concentration could be observed. A more pronounced effect on the particle size can be expected for process parameters besides system composition, e.g. stirrer speed [25], which will not be addressed here.

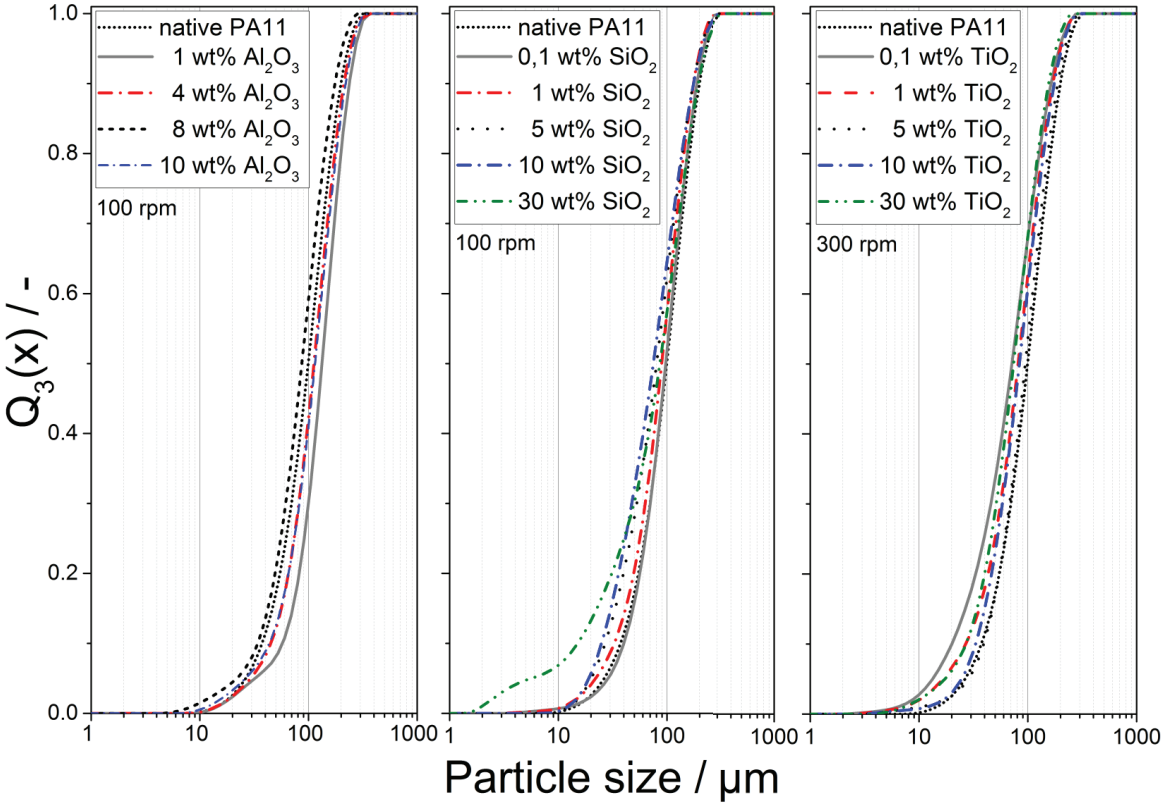

Figure 1: Particle size distribution (volume sum, Q_3) of nanoparticle-filled PA11 particles. Left: Alumina-filled PA11 particles. Middle: Silica-filled PA11 particles. Right: Titania-filled PA11 particles

The effect of the added nanoparticles on the particle shape and morphology can be assessed using SEM imaging. In Figure 2, images of the nanoparticle-filled PA11 particles are depicted. The particle shape in all samples is typical for precipitated PA11 (c.f. [25]), while the surface morphology differs. Due to the different density of the nanoparticles, namely 3.27 g/cm³, 2.2 g/cm³ and 3.5 g/cm³ for alumina, silica and titania respectively, the volume weighted degree of filling varies. This is immanent, when the 30 wt.% samples of silica and titania are compared. The shape and surface morphology of the 30 wt.% titania sample, which

corresponds to around 8.9 vol.%, and the 10 wt.% alumina sample, with 3.2 vol.% alumina, is typical for precipitated PA11. The 30 wt.% silica sample however, with around 14.2 vol.% silica, appears very smooth and completely covered in a nanoparticle shell. With such high degrees of filling, sintering of the particles in the SLS process might be hindered, as the nanoparticles could contribute to a Pickering stabilization at the boundary layer of the molten particles [26] and, thus, inhibit melt coalescence. Regarding SLS processability, nanoparticles could also affect the recrystallization of the polymer after exposure to the laser, as the particles could act as nuclei for heterogeneous nucleation. These effects will be addressed via DSC.

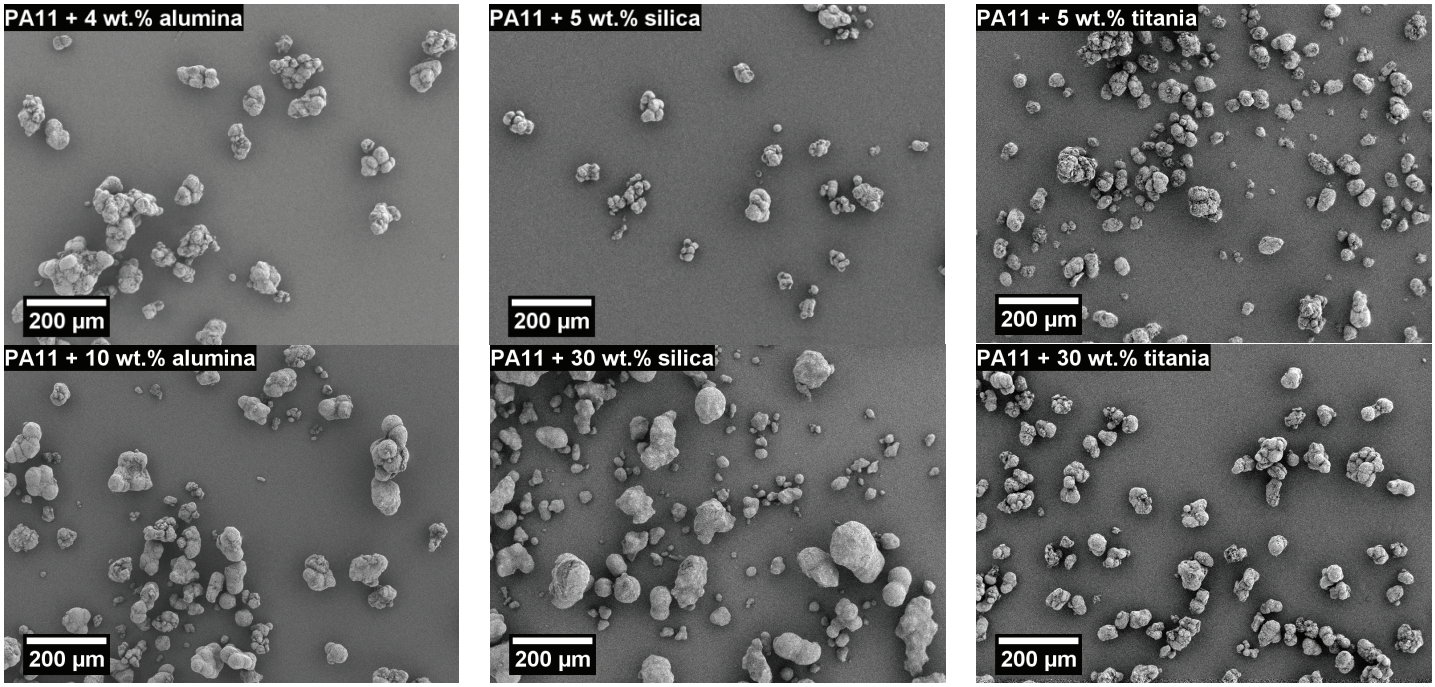

Figure 2: SEM images of nanoparticle-filled PA11 particles.

In order to check, if the desired amount of nanoparticles is incorporated into the particles during the precipitation process, TGA measurements were performed. The quantified ash residue can be correlated to the amount of nanoparticles in the powder sample. Due to post processing, namely washing with ethanol and suction filtering, of the obtained powders after the precipitation process, the occurrence of free nanoparticles in the investigated powders, which are neither enclosed in the polymer particle matrix, nor adhered to the polymer particle surface, is rather unlikely. Since all investigated nanoparticles are oxides, no significant weight change by oxidation or any other change of chemical constitution of the filler during measurement in synthetic air (80 % N_2/20 % O_2) is expected. The quantified ash residue for the nanoparticle-filled powders manufactured under variation of the stirring conditions during precipitation and the added amount of nanoparticles is depicted in Figure 3.

The desired amount of nanofillers, as initially added to the precipitation process, can be found with very good agreement in the powder bulk. Independent of the stirring conditions during precipitation, the desired amount of filler is present in the powder material for all investigated samples. Only for alumina, a slightly higher amount than expected is found in the samples. Since this happens in all samples, a systematic error, e.g. by oxidation, and thereby weight increase, of unreacted species in the pyrogenic alumina or the transition from the oxide to the thermodynamically favored hydroxide is probable. While the TGA measurements show nicely, that it is possible to precisely tailor the amount of nanofillers in the powder with our precipitation approach, no information on the location of the fillers in the powder can be given. It can be assumed that the fillers are incorporated into the particle matrix, since especially for the high filler concentrations, coverage of the polymer particle surface only is unlikely. Furthermore, the presence of free nanoparticles is improbable, as extensive washing and suction filtering of the obtained powder is performed after the initial precipitation experiment.

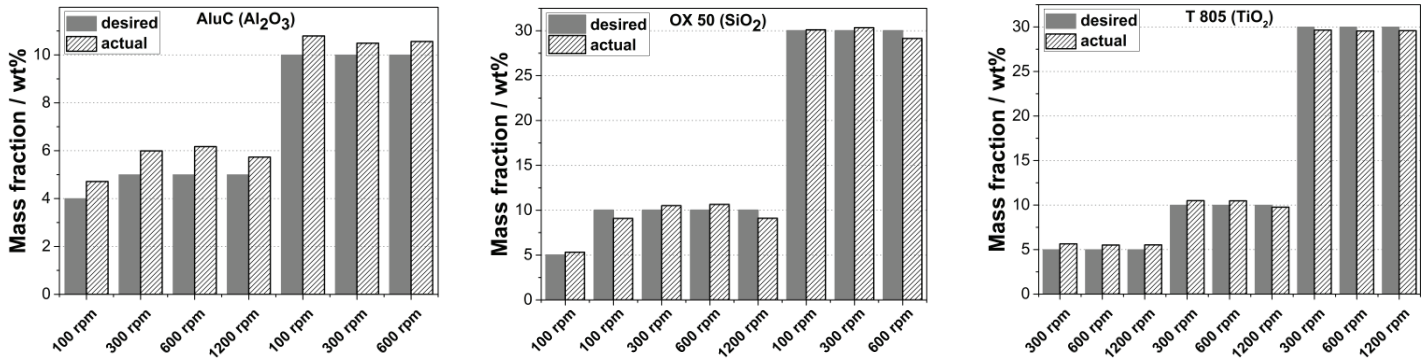

Figure 3: Quantified ash residue for alumina-filled (left), silica-filled (middle) and titania-filled (right) PA11 particles manufactured under variation of stirring conditions.

As an approach to gain information on the distribution of the nanofillers in the particles, polished cross-sections of epoxy-embedded particles were investigated via SEM and EDX analyses, which allows to assess the local chemical identity and spatial distribution of the filler within the polymer matrix. SEM images of the cross-sections are given in Figure 4.

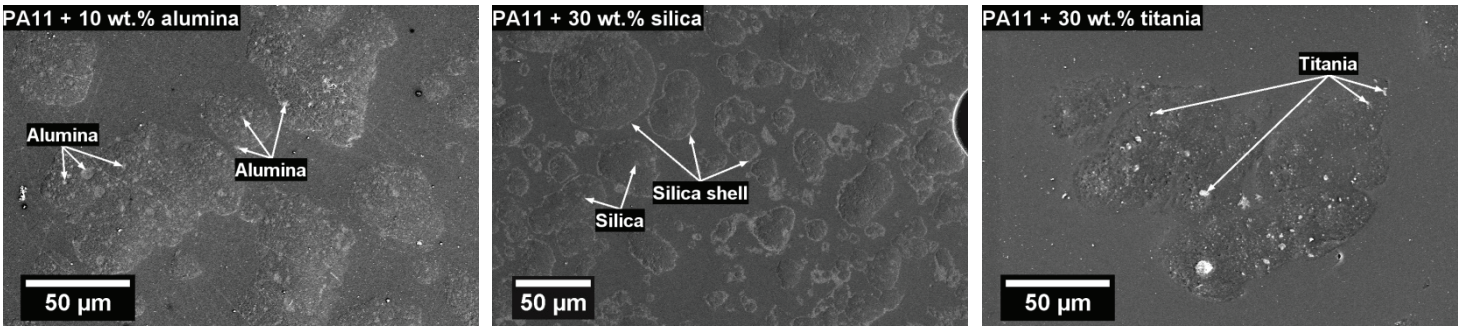

Figure 4: From left to right: Images of cross sections of 10 wt.% alumina-filled, 30 wt.% silica-filled and 30 wt.% titania-filled PA11 particles embedded in resin.

For alumina-filled PA11, an even distribution of smaller and larger nanoparticle agglomerates can be well observed in the polymer particle matrix. The EDX analysis shows a signal at 1.487 keV, which can be attributed to aluminum. In the case of titania, the nanoparticles are visible in the polymer particle matrix for the 30 wt.% sample. Also here, smaller and larger titania agglomerates are distributed in the polymer, which give the unique Ti signal at 4.508 keV. The 30 wt.% silica sample shows a different behavior: While there are also silica particles present in the particle matrix, compared to the other samples, more silica nanoparticles, with a signal at 1.740 keV, can be found at the polymer particle surface. This silica shell can be seen in Figure 4 for the silica sample as a bright outline of the slightly darker particle matrix. This corresponds well to the observations made via SEM imaging of the 30 wt.% silica-filled PA11 composite powder, where a shell-like silica layer on the particle surface could be observed. It should be mentioned, that naturally only larger nanoparticle agglomerates can be readily observed in the SEM with the employed imaging settings. However, in all samples, the incorporation of nanoparticles into the polymer particle matrix could be shown. Such observations hint at the interaction and adhesion of the nanofillers with the polymer matrix. However, as mechanical properties of laser sintered nanocomposites are, in addition to filler concentration, governed by the distribution and bonding of the fillers in and on the polymer, thorough specimen characterization must be subject of future studies.

To determine the effect of the filler nanoparticles on the thermal properties (e.g. the ‘sintering window’), DSC experiments were conducted. The thermograms for the alumina-, silica- and titania-filled PA11 are depicted in Figure 5. A detailed discussion on the thermograms and the occurring double α-phase melt endotherm for the first heating of precipitated PA11 can be found in [25]. Interestingly, silica does hardly influence the crystallization of PA11, as no shift in the crystallization peak is observable, even though silica

provides the highest volume concentration of the investigated nanoparticles. The added silica nanoparticles do not act as nucleating agents, thus no premature crystallization is induced. This observation supports the widespread use of pyrogenic silica as flowability enhancers for SLS powders, as no negative impact on the sintering window is to be expected, especially given the typically low concentrations (0.1 wt.% - 0.5 wt.%) used [27–29]. Furthermore, no significant decrease or increase of the crystallinity (as determined from the melting peak using a melt enthalpy of a perfect PA11 crystal of 189.05 J/g [30]) could be observed. While the precipitated native PA11 powder shows a crystallinity of 63 %, all silica-filled samples are in a range of ± 5 %, when corrected for the added silica mass fraction. Contrary to Chunze et al. [21], the employed silica in this study does not lead to a narrowing of the sintering window, which is beneficial for SLS processing.

However, titania with the lowest volume concentration, shows a drastic increase of the crystallization onset from 169.7 °C for native PA11 to 170.9 °C, 174.1 °C, 175.8 °C, 177.2 °C and 179.4 °C for titania concentrations of 0.1 wt.%, 1 wt.%, 5 wt.%, 10 wt.% and 30 wt.%, respectively. Addition of only 0.1 wt.% titania already results in a shift of the crystallization onset of around 1 °C , while 30 wt.% lead to a shift of 10 K. Based on this observation, addition of titania of this grade as a whitening agent for SLS materials should be considered carefully, as a strong decrease of the thermal sintering window is to be expected.

Addition of alumina leads also to an increase of the crystallization onset, however, not as pronounced as titania. The crystallization onset is shifted from 169.7 °C for native PA11 powder to 171.1 °C, 170.7 °C, 173.5 °C and 173.6 °C for alumina concentrations of 1 wt.%, 4 wt.%, 8 wt.% and 10 wt.%, respectively. Such a behavior has been reported previously for PA11-alumina nanocomposites [23]. Compared to titania, the addition of 10 wt.% of alumina leads only to an increase of the crystallization onset of around 4 K instead of 8.5 K.

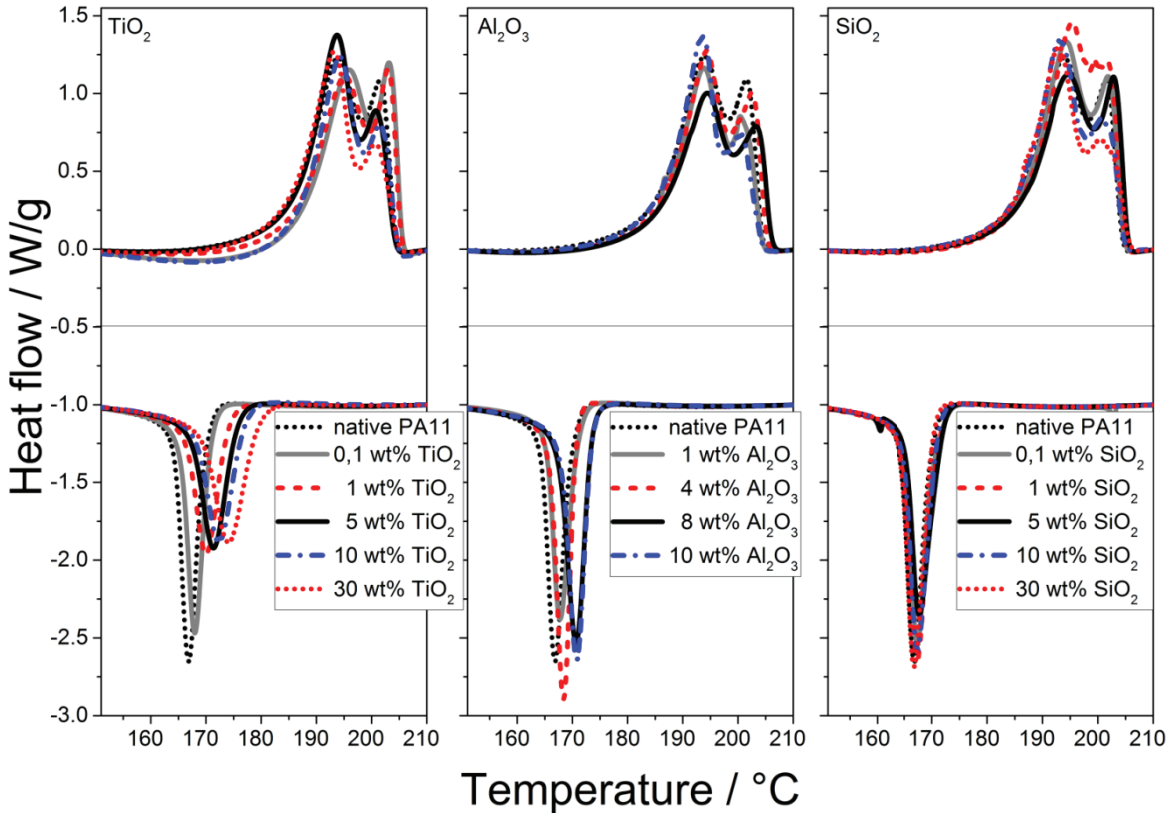

Figure 5: First heating and cooling thermograms of nanoparticle-filled PA11 powders with varying concentrations of titania, alumina and silica, respectively.

Since the observed effect of crystallization onset shift cannot be linked to sheer number or volume concentration of nanoparticles present in the PA11, IGC measurements of the native PA11 powder and the pure nanoparticles were performed. Via IGC, the surface energy of the powders is accessible and by comparing the energies, there might be some correlations between the effect or non-effect as nucleating agents of the investigated nanoparticles for PA11. IGC measurements have been shown to be viable to investigate adhesion

in polymer-fiber composites [31,32]. The determined components of polar and disperse surface energy are depicted in Figure 6 left and right, respectively.

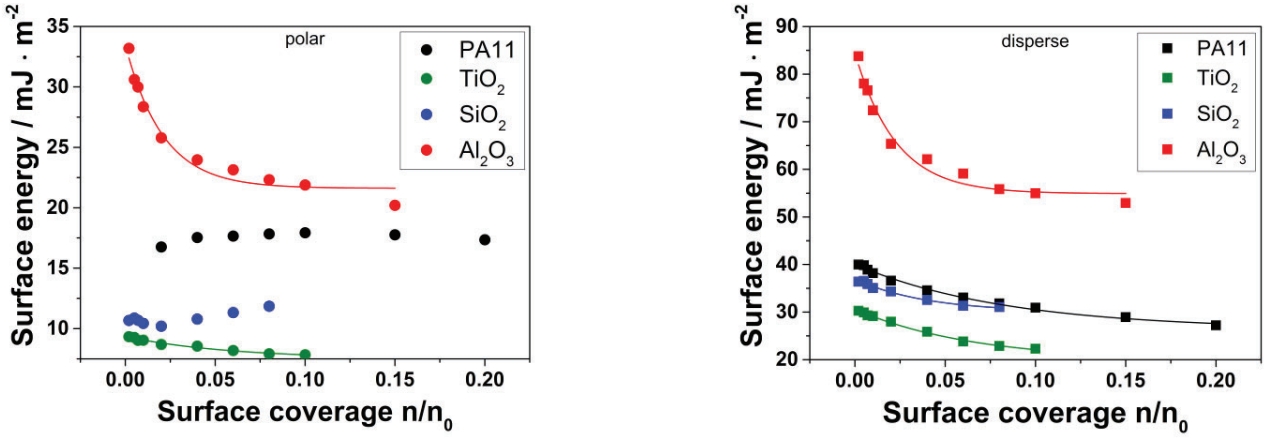

Figure 6: Plot of the polar (left) and disperse (right) components of the surface energies of PA11, titania, silica and alumina, as determined by IGC.

The IGC measurements show, that the polar and disperse surface energy components of titania are lower than those of PA11. For alumina, both components show significantly higher surface energies than PA11, especially concerning disperse surface energies. While the polar surface energy component of silica is lower than PA11, the disperse component is nearly similar to that of PA11. While the small difference in the disperse surface energy between PA11 and silica might be linked to the weak nucleating effect observed via DSC, no such correlations can be drawn easily for the strong nucleating effect of titania and the minor effect of alumina. While alumina is the only investigated material with higher polar and disperse surface energy components and additionally shows the highest energy difference to PA11, its nucleating effect is significantly less pronounced than that of titania. Based on these observations, no direct correlation can be drawn from surface energy measurements and possible effects as nucleating agents in these investigated systems. However, when looking at Hamaker constants of the filler materials, which are represented in the disperse surface energy, a trend can be observed. Ackler et al. [33] give vacuum Hamaker constants for the ceramic filler materials determined by different measurement techniques. The mean values over the different techniques are 61.8 zJ ± 4 zJ, 137.0 zJ ± 12.8 zJ and 300.8 zJ ± 115.5 zJ, for silica, alumina and titania, respectively, which follows the observed effectiveness as nucleating agent. However, the reason for our deviating results obtained from IGC might stem from the precursor-induced organic residues and surface groups present on pyrogenic oxide materials, which often determine the specific field of application of the nanoparticles [34]. As the measurements were conducted with pristine material at 50 °C, the effect of the solution-dissolution process on the surface groups remains unknown. Further investigations are needed to shed more light on the topic.

Conclusion

In this study, we could show the manufacturing of nanoparticle-filled PA11 powder materials with tailored filler concentration for application in laser sintering. Shape and size, especially after appropriate classification, of the manufactured particles are suitable for SLS processing. Via TGA, we could show that almost complete incorporation of the filler material added during the precipitation process is possible, thus enabling tailoring of the filler content. This is important, as previous studies showed that resulting properties of laser sintered specimen depend on filler concentration [22]. Furthermore, we could show, that the fillers are incorporated into the particle volume, thus our process yields true polymer-nanofiller composite particles, contrary to physical mixtures, where the nanoparticles remain on the polymer surface [23]. While the added nanoparticles did not remarkably influence particle size, a huge impact on the thermal sintering window and especially the crystallization was observable, thus directly influencing SLS processability. Interestingly, silica, which is often used as a flowability enhancer, did not act as a nucleating agent for PA11, even at concentrations

as high as 30 wt.%. The added titania led to a drastic increase of crystallization onset and, thereby, a narrowing of the sintering window. Therefore, the addition of titania as e.g. whitening agent should be considered carefully. Although the effects in DSC were well observable, no direct correlation between surface energy as obtained via IGC and nucleating effect could be drawn. For future investigations, powder processability must be addressed. Based on that, concentration-dependent part properties and maximum filling degrees, where sintering of the particles is still possible and, thus, stable parts are obtainable via SLS, shall be assessed.

Acknowledgement

This study has been funded by the Deutsche Forschungsgemeinschaft (DFG, German Research Foundation) – Project-ID 61375930 – SFB 814, Subproject A1, A3 and A6. The financial support is gratefully acknowledged.

References

[1] I. Gibson, D. Rosen, B. Stucker, Additive manufacturing technologies, 2. ed., Springer, New York, NY, 2015.
[2] T.T. Wohlers, Wohlers Report 2016, Wohlers Associates, Fort Collins, Col., 2016.
[3] A.C. Balazs, T. Emrick, T.P. Russell, Nanoparticle Polymer Composites: Where Two Small Worlds Meet, Science (80-.). 314 (2006) 1107–1110.
[4] C. Zhao, P. Zhang, G. Chen, X. Wang, Rheological behavior of novel polyamide 6/silica nanocomposites containing epoxy resins, J. Cent. South Univ. Technol. 15 (2008) 76–79. doi:10.1007/s11771-008-0318-y.
[5] L. Incarnato, P. Scarfato, L. Scatteia, D. Acierno, Rheological behavior of new melt compounded copolyamide nanocomposites, Polymer. 45 (2004) 3487–3496. doi:10.1016/j.polymer.2004.03.005.
[6] D. Arencón, J.I. Velasco, Fracture toughness of polypropylene-based particulate composites, Materials (Basel). 2 (2009) 2046–2094. doi:10.3390/ma2042046.
[7] A. Adnan, C.T. Sun, H. Mahfuz, A molecular dynamics simulation study to investigate the effect of filler size on elastic properties of polymer nanocomposites, Compos. Sci. Technol. 67 (2007) 348–356. doi:10.1016/j.compscitech.2006.09.015.
[8] S. Yuan, F. Shen, C.K. Chua, K. Zhou, Polymeric composites for powder-based additive manufacturing: Materials and applications, Prog. Polym. Sci. (2018). doi:10.1016/j.progpolymsci.2018.11.001.
[9] J. Schmidt, J. Gómez Bonilla, M. Sachs, L. Lanzl, K. Wudy, K.-E. Wirth, D. Drummer, W. Peukert, Production of polybutylene terephthalate glass composite powders and characterization for processing in selective laser sintering, in: Proc. 26th Annu. Int. Solid Free. Fabr. Symp., 2016: pp. 989–997.
[10] S. Kloos, W. Peukert, J. Schmidt, Production of polymer agglomerates by spray drying, in: Proc. 6th Int. Conf. Addit. Technol., 2016: pp. 147–151.
[11] K. Wudy, L. Lanzl, D. Drummer, Selective laser sintering of filled polymer systems: Bulk properties and laser beam material interaction, Phys. Procedia. 83 (2016) 991–1002. doi:10.1016/j.phpro.2016.08.104.
[12] M. Schmid, Laser Sintering with Plastics, Carl Hanser Verlag GmbH & Co. KG, München, 2018.
[13] S.C. Ligon, R. Liska, J. Stampfl, M. Gurr, R. Mülhaupt, Polymers for 3D Printing and Customized Additive Manufacturing, Chem. Rev. 117 (2017) 10212–10290. doi:10.1021/acs.chemrev.7b00074.
[14] P. van de Witte, P.J. Dijkstra, J.W.A. van den Berg, J. Feijen, Phase separation processes in polymer solutions in relation to membrane formation, J. Memb. Sci. 117 (1996) 1–31. doi:10.1016/0376-7388(96)00088-9.
[15] K.S. McGuire, A. Laxminarayan, D.R. Lloyd, Kinetics of droplet growth in liquid-liquid phase separation of polymer-diluent systems: experimental results, Polymer. 36 (1995) 4951–4960. doi:10.1016/0032-3861(96)81620-X.
[16] G. Rehage, D. Möller, O. Ernst, Entmischungserscheinungen in lösungen von molekularuneinheitlichen hochpolymeren, Die Makromol. Chemie. 88 (1965) 232–255. doi:10.1002/macp.1965.020880115.
[17] S. Kloos, M.A. Dechet, W. Peukert, J. Schmidt, Production of spherical semi-crystalline polycarbonate microparticles for Additive Manufacturing by liquid-liquid phase separation, Powder Technol. 335 (2018). doi:10.1016/j.powtec.2018.05.005.

[18] H. Matsuyama, M. Teramoto, M. Kuwana, Y. Kitamura, Formation of polypropylene particles via thermally induced phase separation, Polymer. 41 (2000) 8673–8679. doi:10.1016/S0032-3861(00)00268-8.
[19] S.-J. Wang, J.-Y. Liu, L.-Q. Chu, H. Zou, S.-J. Zhang, C.-J. Wu, Preparation of polypropylene microspheres for selective laser sintering via thermal-induced phase separation: Roles of liquid-liquid phase separation and crystallization, J. Polym. Sci. Part B Polym. Phys. 55 (2017) 320–329. doi:10.1002/polb.24275.
[20] J. Kim, T.S. Creasy, Selective laser sintering characteristics of nylon 6/clay-reinforced nanocomposite, Polym. Test. 23 (2004) 629–636. doi:10.1016/j.polymertesting.2004.01.014.
[21] Y. Chunze, S. Yusheng, Y. Jinsong, L. Jinhui, A nanosilica/nylon-12 composite powder for selective laser sintering, J. Reinf. Plast. Compos. 28 (2009) 2889–2902. doi:10.1177/0731684408094062.
[22] H. Chung, S. Das, Functionally graded Nylon-11/silica nanocomposites produced by selective laser sintering, Mater. Sci. Eng. A. 487 (2008) 251–257. doi:10.1016/j.msea.2007.10.082.
[23] A. Warnakula, S. Singamneni, Selective laser sintering of nano Al2O3 infused polyamide, Materials (Basel). 10 (2017). doi:10.3390/ma10080864.
[24] F.E. Baumann, S. Monsheimer, M. Grebe, W. Christoph, T. Schiffer, H. Scholten, Laser-sintering powder containing titanium dioxide particles, process for its preparation, and moldings produced therefrom, US7148286B2, 2006.
[25] M.A. Dechet, A. Goblirsch, S. Romeis, M. Zhao, F.J. Lanyi, J. Kaschta, D.W. Schubert, D. Drummer, W. Peukert, J. Schmidt, Production of polyamide 11 microparticles for Additive Manufacturing by liquid-liquid phase separation and precipitation, Chem. Eng. Sci. 197 (2019) 11–25. doi:10.1016/j.ces.2018.11.051.
[26] S.A.F. Bon, The Phenomenon of Pickering Stabilization: A Basic Introduction, Part. Emuls. Colloids Form. Appl. 13 (2014) 298–302. doi:10.1595/205651315X689126.
[27] M.M. Lexow, D. Drummer, New Materials for SLS: The Use of Antistatic and Flow Agents, J. Powder Technol. 2016 (2016) 1–9. doi:10.1155/2016/4101089.
[28] J. Schmidt, M. Sachs, S. Fanselow, M. Zhao, S. Romeis, D. Drummer, K.E. Wirth, W. Peukert, Optimized polybutylene terephthalate powders for selective laser beam melting, Chem. Eng. Sci. 156 (2016) 1–10. doi:10.1016/j.ces.2016.09.009.
[29] C. Blümel, M. Sachs, T. Laumer, B. Winzer, J. Schmidt, M. Schmidt, W. Peukert, K.-E. Wirth, Increasing flowability and bulk density of PE-HD powders by a dry particle coating process and impact on LBM processes, Rapid Prototyp. J. 21 (2015) 697–704. doi:10.1108/RPJ-07-2013-0074.
[30] Q. Zhang, Z. Mo, S. Liu, H. Zhang, Influence of annealing on structure of Nylon 11, Macromolecules. 33 (2000) 5999–6005. doi:10.1021/ma000298d.
[31] R.T. Pogue, J. Ye, D.A. Klosterman, A.S. Glass, R.P. Chartoff, Evaluating fiber–matrix interaction in polymer–matrix composites by inverse gas chromatography, Compos. Part A Appl. Sci. Manuf. 29 (1998) 1273–1281. doi:10.1016/S1359-835X(98)00074-8.
[32] D. Williams, Characterisation of Filler and Fibre Surfaces Using Inverse Gas Chromatography, in: Hatsuo Ishida (Ed.), Proc. Third Int. Conf. Compos. Interfaces, Springer Netherlands, Cleveland, Ohio, USA, 1990: pp. 219–232. doi:10.1007/978-94-011-7816-7_22.
[33] H.D. Ackler, R.H. French, Y.-M. Chiang, Comparisons of Hamaker Constants for Ceramic Systems with Intervening Vacuum or Water: From Force Laws and Physical Properties, J. Colloid Interface Sci. 179 (1996) 460–469. doi:10.1006/jcis.1996.0238.
[34] W.Y. Teoh, R. Amal, L. Mädler, Flame spray pyrolysis: An enabling technology for nanoparticles design and fabrication, Nanoscale. 2 (2010) 1324. doi:10.1039/c0nr00017e.